Modeling the Impact of Roadway Emissions in Light Wind, Stable and Transition Conditions

Akula Venkatram*

University of California, Riverside, CA 92521, USA

Michelle Snyder, Vlad Isakov

US Environmental Protection Agency, Office of Research and Development, National Exposure Research Laboratory, Atmospheric Modeling and Analysis Division, Research Triangle Park, NC 27711, USA

Abstract

This paper examines the processes that govern air pollution dispersion under light wind, stable and transition conditions by using a state-of-the-art dispersion model to interpret measurements from a tracer experiment conducted next to US highway 99 in Sacramento in 1981-82 during the early morning and late evening when winds were light and variable. We examine the roles of stability, wind meander, and boundary layer height on concentrations measured during this study. Our analysis suggests that currently used equations for vertical plume spread need modification when the winds are light. The shallow boundary layer associated with these conditions limits vertical mixing and hence reduces the rate at which concentrations fall off with distance from the road.

Keywords: Air quality, roadway emissions, dispersion modeling, low wind speeds, tracer experiment

1. Introduction

The impact of roadway emissions on air quality has become prominent in the light of recent epidemiological studies reporting associations between living within a few hundred meters of high-traffic roadways and adverse health effects such as asthma and

* Corresponding author: venky@engr.ucr.edu; venkatram@sbcglobal.net

other respiratory impacts, birth and developmental effects, premature mortality, cardiovascular effects, and cancer. This paper examines the processes that govern dispersion of roadway emissions during stable and transition periods when the near surface winds are light and variable, and then suggests improvements to currently used dispersion models.

2. Caltrans Highway 99 Tracer Experiment

This tracer study was conducted by Caltrans during the winter of 1981-82 along a 4 km section of US. Highway 99 in Sacramento (Benson, 1989). This section of the highway runs along the northwest-southeast direction, as shown in Figure 1. The nearby terrain consists of open fields and parks to the north, and scattered residential developments to the south. The highway has two lanes in each direction separated by a 14 meter median. It carries over 35,000 vehicles daily with a peak hourly count of 3,450.

The tracer, sulfur hexafluoride, $SF_{6,}$ was released into the exhaust stream of eight specially equipped 1970 Matador sedans. These automobiles circulated up and down the highway, beginning one hour before sampling started. Half of the vehicles were driven in the right hand lane and the other half in the left to distribute the emissions evenly across the lanes of the highway. The vehicles released SF_6 along the 4 km test section on both the departing and return legs of the loop. Each vehicle was allowed 12 minutes to complete the loop. The distribution of the vehicles was controlled at the staging area by spacing departures 1.5 minutes apart. This meant that, on average, a 4 km release was started every 45 seconds.

Tests were three hours long, with samples taken during the last two hours. The one hour delay is to avoid sampling during the transient build-up phase of the release. SF_6 monitors were arrayed on both sides of the road at 50, 100 and 200m from the center, and at four locations along the median (spaced roughly 800 m apart) (Figure 1). Samplers were positioned 1m above ground level. Samples were collected in Tedlar bags for four consecutive 30-minute periods and analyzed with gas chromatography. Two cup and vane anemometers were installed on a 12 m meteorological tower near the sampling array at heights of approximately 6.5 m and 11.4 m.

Fourteen tracer release tests were conducted. All but three of these were morning tests with samples taken from 6:30 to 8:30 a.m. PST in most cases. Two of the three afternoon runs took place from 4:00 to 6:00 p.m. The remaining afternoon run was made from 5:00 to 7:00 p.m. Traffic counts and classifications were made concurrently with the aerometric measurements for many of the test runs.

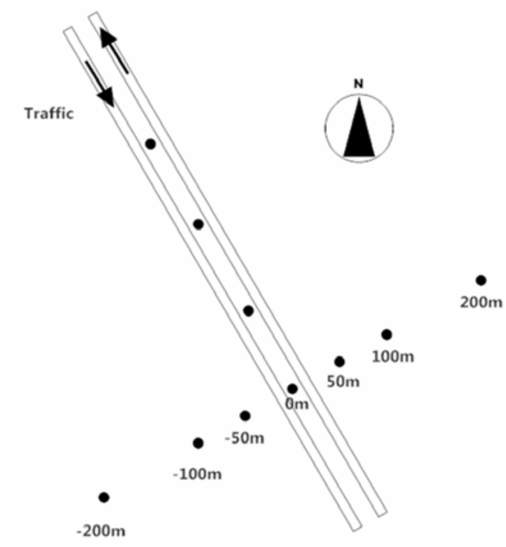

Figure 1. Schema of layout of Caltrans highway 99 tracer study.

We first examine the behavior of the measured concentrations downwind of the road as a function of wind speed and direction. Figure 2 shows that the concentration increases as the wind speed decreases, a trend most clearly seen at the median. Figure 3 shows that wind direction ranges over 0 to 90 degrees during, and that the concentrations are insensitive to the wind direction at all four downwind receptors. This insensitivity to wind direction agrees with our theoretical understanding of dispersion from line sources (Venkatram and Horst, 2006).

Figure 4 shows that concentration falls off rapidly from its maximum at the median to about half of the maximum at 50 m. Thereafter, the concentration variation is relatively slow decreasing from about a mean of 1000 μgm^{-3} at 50 m to about 500 μgm^{-3} at 200

m. The mean vertical spread of the plume, estimated from the measured concentrations, increases rapidly at first and then levels off at around 15 m. This suggests that the vertical spread is limited by a shallow boundary layer.

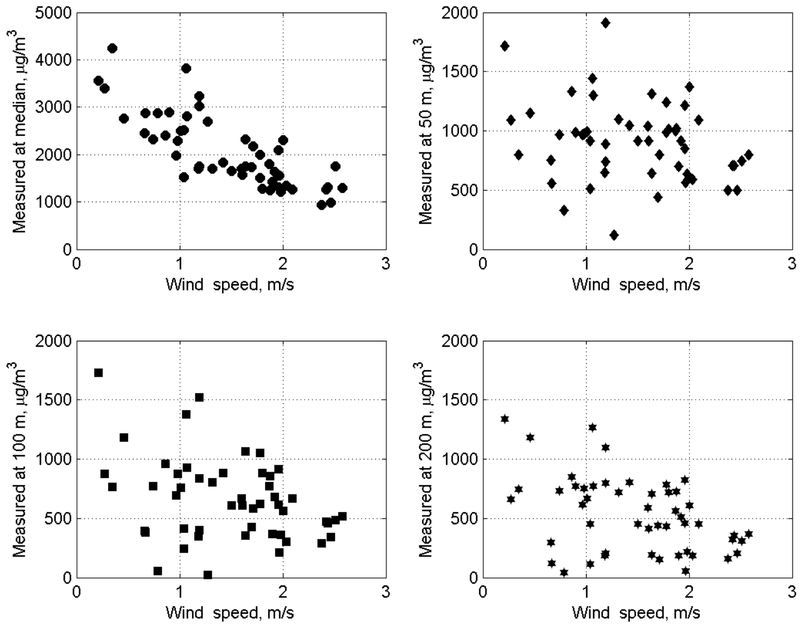

Figure 2: Variation of concentrations with wind speed at 11.4 m at downwind receptors

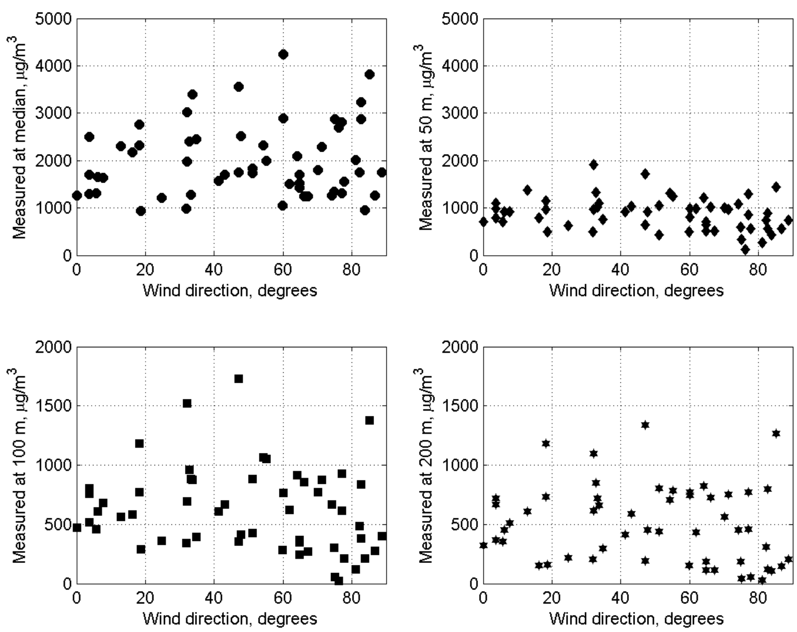

Note: 90^0 corresponds to wind direction parallel to the road.

Figure 3: Variation of concentrations with wind direction relative to road normal at downwind receptors.

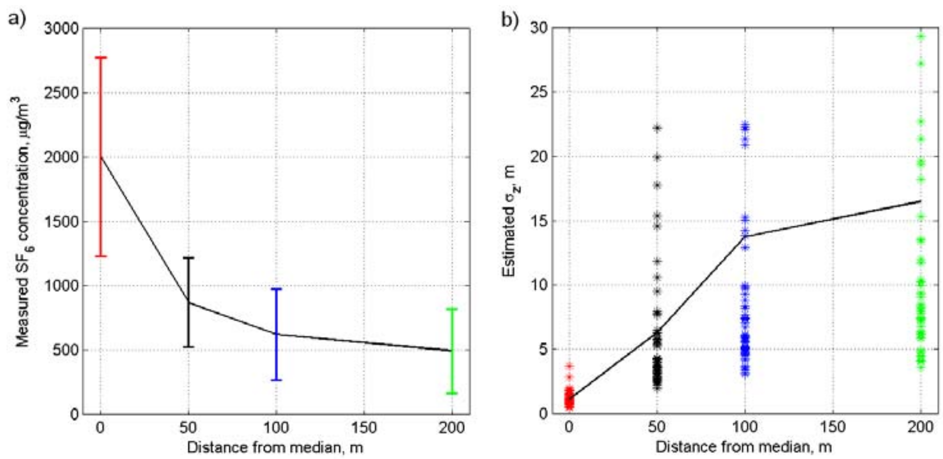

Note: The left panel shows the mean ± standard deviation of the concentrations at each distance. The solid line in the left panel is drawn through the mean of the concentrations at each distance.

Figure 4: Variation of concentrations and estimated plume spreads with distance from median.

3. Dispersion Model

The freeway is represented as four line sources located at the center of each lane of the freeway. Each line source is modeled is represented as a set of elemental point sources, as shown in Figure 5. The contribution of the elemental point source, *dC*, located at $(0, Y_s)$ to the concentration at (X_r, Y_r, Z_r) is given by the Gaussian plume formulation,

$$dC = \frac{q dY_s}{2\pi U \sigma_y(x_r)\sigma_z(x_r)} \exp\left(-\frac{y_r^2}{2\sigma_y^2(x_r)}\right) F(Z_r) \quad , \tag{1}$$

where $F(Z_r)$ is the vertical distribution function given by

$$F(Z_r) = \exp\left(-\frac{(h_s - Z_r)^2}{2\sigma_z^2}\right) + \exp\left(-\frac{(h_s + Z_r)^2}{2\sigma_z^2}\right), \tag{2}$$

where σ_y and σ_z are the horizontal and vertical plume spreads, which are functions of x_r, the receptor's downwind distance in the co-ordinate system aligned with the wind direction, as shown in Figure 5. The second term on the right hand side of Equation 2 accounts for plume reflection from the ground.

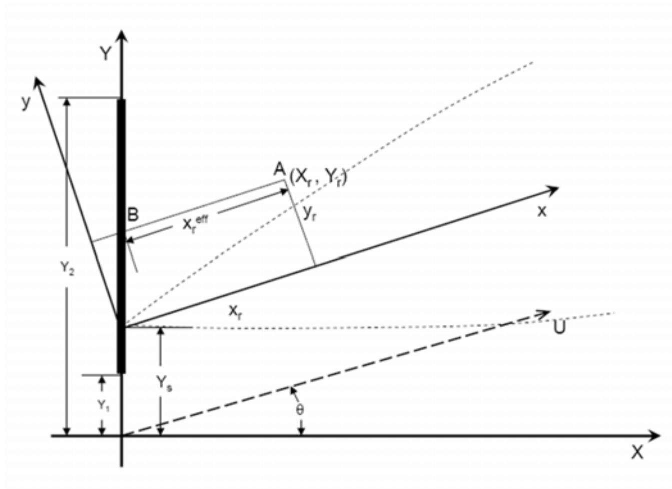

Note: The system x-y has the x-axis along the mean wind direction, which is at an angle θ to the fixed X axis. The dotted line represents the plume originating from an elemental point source at $(0,Y_s)$

Figure 5: Co-ordinate systems to calculate contribution of point source at Y_s to concentration at (X_r,Y_r).

The vertical spread of the plume, σ_z, from each point source is described by equations used in AERMOD (Cimorelli et al., 2005), which is representative of the current generation of dispersion models:

$$\begin{aligned}\sigma_z &= \sqrt{\frac{2}{\pi}}\frac{u_* x_r}{U}\left(1+0.7\frac{x_r}{L}\right)^{-1/3} \quad L>0.0 \\ &= \sqrt{\frac{2}{\pi}}\frac{u_* x_r}{U}\left(1+0.006\left(\frac{x_r}{|L|}\right)^2\right)^{1/2} \quad L<0.0\end{aligned}, \tag{3}$$

where L is the Monin-Obukhov length defined by $L = -T_0 u_*^3/(\kappa g Q_0)$, where Q_0 is the surface kinematic heat flux, u_* is the surface friction velocity, g is the acceleration due to gravity, T_0 is a reference temperature, and κ is the Von Karman constant taken to be 0.40. Equation 3 is a semi-empirical formulation (Venkatram, 1992) based on eddy diffusivity and wind speed profiles derived from Monin-Obukhov (MO) Similarity Theory (Businger, 1971).

The horizontal spread of the plume is based on that in AERMOD (Cimorelli et al., 2005):

$$\sigma_y = \frac{\sigma_v x_r}{U}\left(1+78X\right)^{-0.3}$$
$$where \qquad (4)$$
$$X = \frac{\sigma_v x_r}{U z_i}$$

Here σ_v is the standard deviation of the crosswind velocity fluctuations, and z_i is the mixed layer height.

The contribution of a line source to the concentrations at a receptor $(X_r,\ Y_r)$ is given by the integral of the contributions the point sources along the line,

$$C\left(X_r, Y_r\right) = \int_{Y_1}^{Y_1+L} dC \quad . \qquad (5)$$

This integral can be integrated numerically but the computational cost becomes unmanageable if we have to estimate the impact of the large number of roads typical of an urban area. So the model is based on an analytical approximation to the integral, given by Venkatram and Horst (2006),

$$C_p\left(X_r, Y_r\right) \approx \frac{qF(Z_r)}{\sqrt{2\pi}U\sigma_z\left(x_r^{eff}\right)\cos\theta}\left[erf\left(t_1\right) - erf\left(t_2\right)\right] \quad . \qquad (6)$$

where

$$x_r^{eff} = X_r / \cos\theta \quad , \qquad (7)$$

$$t_i = \frac{\left(Y_r - Y_i\right)\cos\theta - X_r \sin\theta}{\sqrt{2}\sigma_y\left(x_i\right)}, \qquad (8)$$

where q is the emission rate per unit length of the line source. Here σ_y is evaluated at $x_i \equiv x_r\left(Y_s = Y_i\right)$. The definitions of t_1 and t_2 correspond to downwind distances, x_r, from the end points Y_1 and Y_2 of the line to the receptor at $(X_r,\ Y_r)$. We see from Figure 5 that the vertical spread in Equation 6 is evaluated at a downwind distance from the line source along the wind direction.

The CAR-FMI model (Kukkonen et, 2001) uses a formulation similar to Equation 6. It is based on an approximation to Equation 5 from Luhar and Patil (1989), which evaluates both horizontal and vertical plume spreads at the effective downwind distance, $X_r/\cos\theta$. Venkatram and Horst (2006) show that the LP formulation has large errors relative to the numerically evaluated value beyond wind angles of about 70^0 from the road normal. The HV approximation, which evaluates the horizontal spread at effective distances measured from the ends of the road, is accurate at angles close to 90^0. However, even this approximation breaks down at $\theta = 90^0$ because of the term $cos\theta$ in the denominator of Equation (6). CAR-FMI avoids this singularity by adding a constant of 0.2 m/s to the wind speed based on a suggestion by Luhar and Patil (1989).

We avoid the problem at $\theta = 90^0$ by taking $\sigma_z\left(\frac{X_r}{cos\theta}\right)cos\theta$=$\sigma_z(X_r)$ in the denominator of Equation 6. This limit is consistent with the exact solution of the integral for a parallel wind when the vertical and horizontal plume spreads are linear with downwind distance. We account for this limit by setting the denominator in the equation to $(\sigma_z(X_r) + \sigma_z(X_r/cos\theta)cos\theta)/2$. Comparison with the numerical solution indicates that this approach has an error of less than 25% when θ approaches 90^0.

Under low wind speeds, horizontal meandering of the wind spreads the plume over large azimuth angles, which leads to concentrations at receptors upwind relative to the vector averaged wind direction. AERMOD (Cimorelli et al., 2005), and other currently used regulatory models (e.g. ADMS (Atmospheric Dispersion Modeling System, Carruthers *et al*., 1994), attempt to treat this situation by assuming that when the mean wind speed is close to zero, the horizontal plume spread covers 360°. If the release - spreads radially in all horizontal directions, the concentration from a point source with an emission rate, *Q*, is given by:

$$C(x,y)=\sqrt{\frac{2}{\pi}}\frac{Q}{2\pi rU_e\sigma_z(r)}, \tag{9}$$

where r the distance between the source and receptor and the plume spread covers 2π radians. The plume is transported at an effective velocity given by

$$U_e=\left(\sigma_u^2+\sigma_v^2+U^2\right)^{1/2}=\left(2\sigma_v^2+U^2\right)^{1/2}, \tag{10}$$

where U is the mean vector velocity, and the expression assumes that $\sigma_v \approx \sigma_u$.

If we assume that the vertical plume spread is linear with distance, the integral of the contributions of the meandering components of the point sources along the line source can be written as

$$C_m\left(X_r,Y_r\right)=\sqrt{\frac{2}{\pi}}\frac{qF(Z_r)}{U\sigma_z\left(X_r\right)}\frac{\theta_s}{2\pi}. \tag{11}$$

where θ_s is the angle subtended by the line source at the receptor,

$$\theta_s=tan^{-1}\left(\frac{Y_2-Y_r}{X_r}\right)+tan^{-1}\left(\frac{Y_r-Y_1}{X_r}\right). \tag{12}$$

We assume that Equation (11) is a useful approximation even when vertical plume spread is not linear. Note that θ_s is the angle subtended by the line source at the receptor. So the maximum value of this subtended angle is π when the receptor is very close to the line.

We estimated σ_v from the approximation (Cirillo and Poli, 1992)

$$\sigma_v^2=u^2\,sinh\left(\sigma_\theta^2\right), \tag{13}$$

where σ_θ is the measured standard deviation of the horizontal wind direction fluctuations.

Then, the concentration at a receptor is taken to be a weighted average of concentrations of two possible states: a random spread state, Equation 11, and a plume state, Equation 6.

$$C=C_p\left(1-f_r\right)+C_mf_r. \tag{14}$$

The weight for the random component in Equation (14) is taken to be

$$f_r=\frac{2\sigma_v^2}{U_e^2}, \tag{15}$$

This ensures that the weight for the random component goes to unity when the mean wind approaches zero. ADMS uses a weighting scheme based on the mean wind speed.

The need to specify the wind speed, *U*, used in the dispersion model highlights a problem with the application of the Gaussian dispersion equation to releases in the surface layer, where the wind speed varies with height. We compute the wind speed, *U*, at the mean plume height, $\bar{z}$, by solving the following iteratively,

$$\sigma_z = f\left(x, u_*, L, U(\bar{z})\right), \tag{16}$$

where the mean plume height for a Gaussian concentration distribution is given by

$$\bar{z} = \sigma_z \sqrt{\frac{2}{\pi}} exp\left[-\frac{1}{2}\left(\frac{z_s}{\sigma_z}\right)^2\right] + z_s erf\left(\frac{z_s}{\sqrt{2}\sigma_z}\right) \tag{17}$$

where the right hand side of Equation 17 corresponds to the expressions for vertical spread given by Equation 3.

The Caltrans 99 dataset (Benson 1989) does not contain measurements of heat flux, which is required to calculate the MO length, a model input. Here we estimated the micrometeorological inputs required to estimate the plume spreads using the approach described in Cimorelli et al. (2005) which uses the time of day to calculate the solar angle and hence the incoming solar radiation and surface heat flux. We computed the surface friction velocity at low wind speeds under stable conditions using the correction suggested by Qian and Venkatram (2011). The roughness length is taken to be 0.1 m, which provided the best agreement between the friction velocities obtained from the wind speeds measured at the two levels of the tower at 6.5 m and 11.4 m.

4. Evaluation of Dispersion model

We interpret the data from the field study by evaluating modeled estimates of 15-min averaged concentrations at the ten receptors shown in Figure 1 with corresponding observations. The first version of the model neglects the effects that are important under light wind conditions: wind meandering, near-parallel winds, and limited mixing. We will refer to this version as the “unmodified” model.

The performance of the models is quantified using the statistics of the ratio of the modeled, C_p, to the observed concentration, C_o. The first statistic is the median of the ratios, which is denoted by m_g. The second is the fraction of the ratios, C_p/C_o, that lie between 0.5 and 2 of the median value, m_g. This statistic is denoted by *frac2*, and called the factor of two interval.

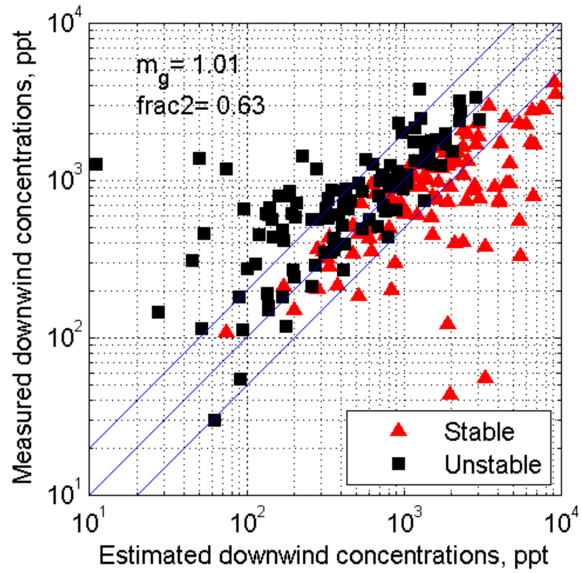

Note: The concentrations along the median are combined into an average.

Figure 6: Comparison of "unmodified"model estimates of SF_6 concentrations with values observed at the receptors shown in Figure 1.

Figure 6 shows results from the unmodified dispersion model, which neglects the effects we consider important under light wind conditions. We see that 63% of the concentrations estimated downwind of the freeway are within a factor of two of the observations. The concentrations are overestimated during stable conditions and underestimated during unstable conditions leading to the small overall bias of m_g=1.01.

The overestimation of concentrations during meteorological conditions classified as stable and underestimation during unstable transition conditions is also apparent in the spatial plot of Figure 7. The figure shows that the measured concentrations do not reflect the estimated differences in stability, which indicates that the stability effects based on MO similarity need modification. The concentrations fall off more slowly than the modeled values suggesting that vertical dispersion is limited by the height of the boundary layer.

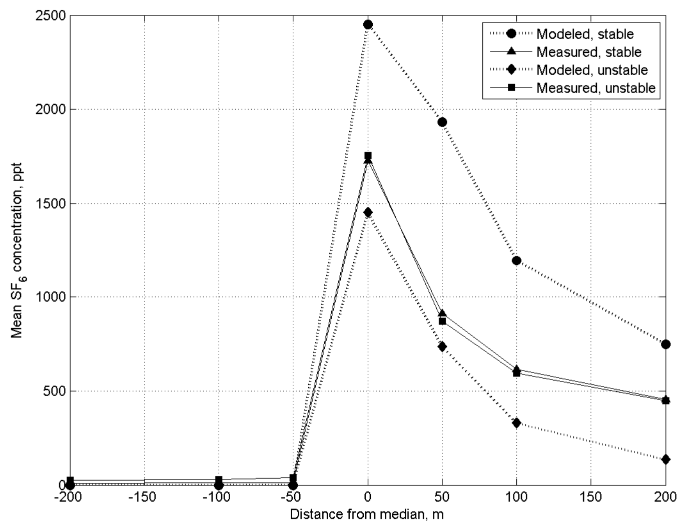

Note: Each point is the median of the modeled and measured values at the receptor.

Figure 7: Spatial variation of modeled and measured concentrations.

The tracer studies were conducted during early morning or late evening hours when the surface boundary layer was undergoing transition from stable to unstable conditions. The wind speeds were also very light. Under these conditions, it is likely that the near surface boundary layer is shallow, unsteady and its structure differs from that described by MO similarity. To examine the sensitivity of the model results to removing this dependence on MO similarity, we set the stability dependent functions in the vertical spread formulations, Equation 3, to unity. In addition we included the following effects that are likely to be important under low wind speeds: vertical mixing limited to 20 m based on observations of σ_z presented in Figure 4, meandering formulation in Equations 11 to 15, and the parallel wind correction. This version of the model represents the "best" attempt to describe dispersion under low, variable winds in stable/transition conditions.

Figure 8 shows that the low wind features improve model performance significantly for downwind concentrations: the factor of two measure increases to 84% and the overall bias is 2%. This improvement is also reflected in the modeled spatial variation shown in Figure 9, although the rate of decrease of the measured concentrations is still smaller than that modeled. The inclusion of meander results in upwind concentrations, which are compared with observations on the right panel of Figure 8. The comparison is poor with the model having a tendency to overestimate concentrations by a factor of 1.67.

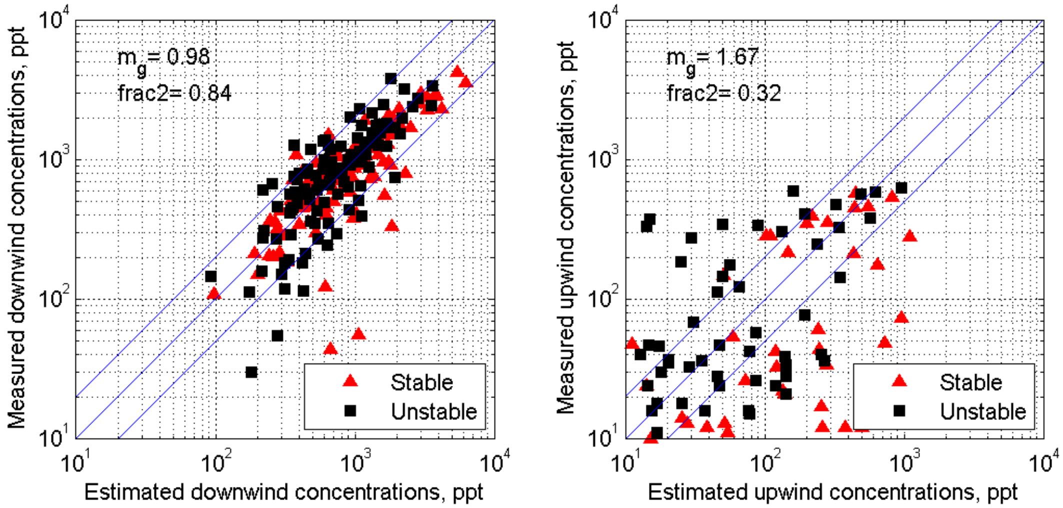

Note: The concentrations along the median of the road are combined into an average.

Figure 8: Comparison of "best" model estimates of SF_6 concentrations with values observed at the receptors shown in Figure 1.

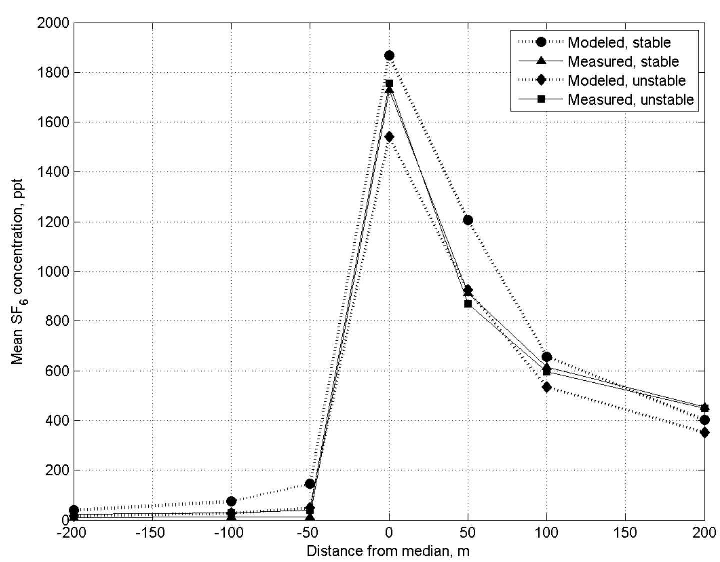

Figure 9: Spatial variation of modeled and measured concentrations when model includes effects associated with low wind conditions.

Figure 10 shows the ratios of the modeled to the measured concentrations as a function of wind direction. The ratios are mostly within the factor of two interval, and are not correlated with the wind direction, a result that supports the treatment of near parallel winds in the model.

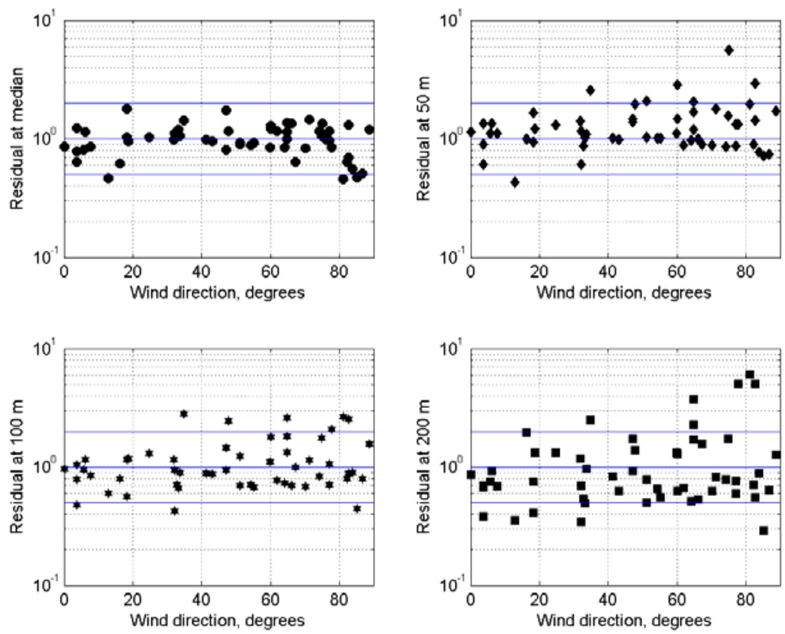

Note: Horizontal lines above and below the unity line correspond to 2 and 0.5, the factor of two interval.

Figure 10: Variation of residual=modeled/measured concentrations as a function of wind direction at 11.4 m relative to normal to the road.

Relative roles of processes governing dispersion

We examined the relative roles of processes governing dispersion under light wind conditions by creating different versions of the model, each of which lacks one of the features we consider important under light wind conditions. A comparison of concentration estimates from each version with observations provides information on the relative importance of the neglected process. A summary of the performance of these versions of the model is depicted in Figure 11 and Table 1.

In Figure 11, the bias is defined as $(m_g - 1) \times 100$. We express model scatter in terms of the fraction of the values of C_p/C_o outside the factor of two interval, $(1\text{-}frac2) \times 100$, where *frac2* is given in Table 1. The length of the line in the figure provides a visual depiction of model performance: model performance deteriorates as the length of the line increases.

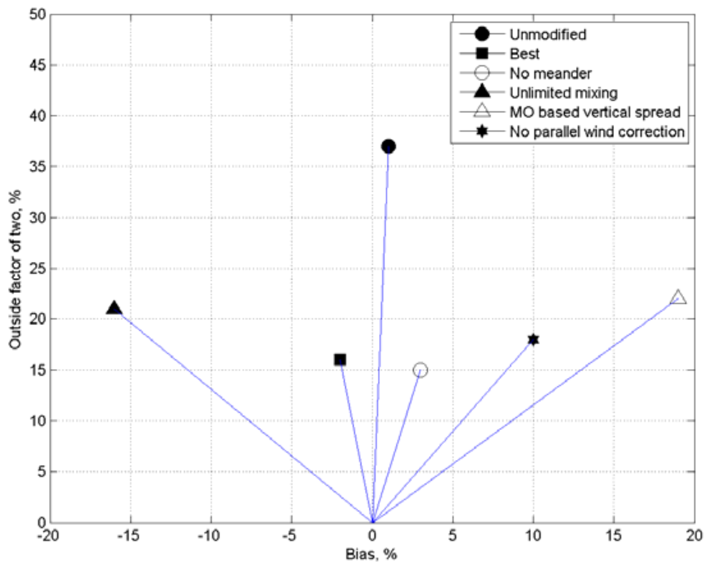

Figure 11: Performance of different versions of the dispersion model.

Table 1: Performance Features of the Dispersion Model

Name	Meander	Parallel Wind Correction	Limited Mixing	MO Stability Included	m_g	frac2 %
Unmodified	No	No	No	Yes	1.01	63
Best	Yes	Yes	Yes	No	0.98	84
No meander	No	Yes	Yes	No	1.03	85
Unlimited mixing	Yes	Yes	No	No	0.84	79
MO based vertical spread	Yes	Yes	Yes	Yes	1.19	78
No parallel wind correction	Yes	No	Yes	No	1.10	82

We see that bias in the unmodified model is small, which is the result of overestimating concentrations during stable conditions and underestimating them during stable conditions; Figure 6. But the scatter is large with close to 37% of the model estimates outside the factor of two interval. The model that includes all the formulations to account for light wind conditions has a scatter of 16%. Neglecting meander makes little difference to model estimates of downwind concentrations. Not accounting for limited vertical mixing results in significant deterioration in model performance relative to the best model: the bias is close to -16% and the scatter is 21% outside the factor of two interval. Assuming that vertical dispersion is based on MO similarity results in overestimation of 19% and a scatter of 22%. Not correcting for near parallel winds results in a bias of 10% and a scatter of 18%.

Conclusions

This paper evaluates our current understanding of dispersion of roadway emissions under light and variable winds in stable/transition conditions by using a model to interpret concentrations measured during a field study conducted during the winter of 1981-82 along a 2.5-mile section of a US. highway focusing on the early morning and late evening when the light and variable winds exacerbated the air quality impact of rush hour traffic. We find that excluding upwind dispersion through meander has a minor impact on the model's ability to describe downwind concentrations. Excluding meander results in zero upwind concentrations, which is not consistent with observations. However, model estimates of upwind concentrations are not in good agreement with observations, which suggests that the current formulation needs to be improved. We find that the excluding the treatment for winds close to parallel to the road leads to overestimation of concentrations, which agrees with results from previous studies. The correction for parallel winds decreases this discrepancy.

Currently used equations used to describe vertical dispersion are sensitive to stability under light wind conditions. Observations do not support this sensitivity because the model provides the best description of the data when the explicit dependence on stability is removed from the equations so that $\sigma_z \propto u_* x / U$. Under light wind, stable or transition periods, the boundary layer, which is likely to be shallow, has a significant impact on near-road concentrations associated with roadway emissions.

Acknowledgements

The authors are grateful to David Heist and Steven Perry of EPA's National Exposure Research Laboratory for useful discussions on the formulation of the line source model, and for their help in constructing meteorological inputs from the Caltrans observations. The US EPA through its Office of Research and Development funded and managed the research, and has been subjected to Agency's administrative review and approved for publication.

References

Benson, P. E. 1989. CALINE4-a Dispersion Model for Predicting Air Pollution Concentration near Roadways. Sacramento, CA: Office of Transportation Laboratory, California Department of Transportation.

Businger, J. A., Wyngaard, J. C., Izumi,Y., Bradley, E.F., 1971. Flux-Profile relationships in the atmospheric surface layer. J. Atmos. Sci., 28, 181-189.

Carruthers, D., Holroyd, R., Hunt, J., Weng, W., Robins, A., Apsley, D., Thompson, D., Smith, F. 1994. UK-ADMS: A new approach to modeling dispersion in the earth's atmospheric boundary layer. *Journal of wind engineering and industrial aerodynamics,* 52, 139-153.

Cimorelli, A.J., Perry, S.G., Venkatram, A., Weil, J.C., Paine, R.J., Wilson, R.B., Lee, R.F., Peters, W.D., Brode, R.W. 2005. AERMOD: A Dispersion Model for Industrial Source Applications. Part I: General Model Formulation and Boundary Layer Characterization. *Applied Meteorology*, 44, 682–693.

Cirillo, M.C. and Poli, A.A. 1992. An intercomparison of semi-empirical diffusion models under low wind speed, stable conditions. *Atmospheric Environment A. General Topics,* 26, 765-774

Kukkonen, J., Harkonen, J., Walden, J., Karppinen, A., Lusa, K. 2001. Evaluation of the CAR-FMI model against measurements near a major road. *Atmospheric Environment,* 35, 949-960.

Luhar, A. K., Patil, R. S. 1989. A General Finite Line Source Model for vehicular pollution prediction. *Atmospheric Environment,* 23, 555-562.

Qian, W., Venkatram, A. 2011. Performance of Steady-State Dispersion Models Under Low Wind-Speed Conditions. *Boundary Layer Meteorology,* 138, 475-491.

Venkatram, A. 1992. Vertical dispersion of ground-level releases in the surface boundary layer. *Atmospheric Environment A,* 26, 947-949.

Venkatram, A., Horst, T., 2006. Approximating dispersion from a finite line source. *Atmospheric Environment*, 40, 2401-2408.